Finite element analyses of concrete penetration with a steel projectile. Comparison of Lagrangian and Eulerian techniques

Paper from: *Structures Under Shock and Impact VII*, N Jones, CA Brebbia and AM Rajendran (Editors).
ISBN 1-85312-911-9

Finite element analyses of concrete penetration with a steel projectile. Comparison of Lagrangian and Eulerian techniques

J. Leppänen, K. Gylltoft
Department of Structural Engineering, Concrete Structures, Chalmers University of Technology, Sweden.

Abstract

When a projectile impacts a concrete target, it penetrates the concrete, severe crushing occurs and a crater forms. When concrete is subjected to impact loading, the strength will increase due to the strain rate and confinement effects. This paper presents finite element analyses of concrete perforation with a steel projectile. To predict the perforation depth of the projectile and the crater size of the concrete, material models are required where the strain rate effect, large deformations and triaxial stress states are taken into account. By using the Lagrangian technique, large deformations will lead to excessive grid distortions and tangling; therefore an erosion algorithm is needed. By using the Eulerian technique, the problems of grid tangling are overcome. The analyses are performed with the nonlinear finite element program AUTODYN and the results are compared to experiments concerning the depth of penetration and the crater diameter.

1 Introduction

1.1 Mesh description

In finite element codes there are two main descriptions for the material movement, i.e. the Lagrange and Euler descriptions as shown in Figure 1. In the Lagrange description, the numerical mesh distorts with the material movement. In the Euler description, the numerical mesh is fixed in space, and the material is moving in the elements. To allow the material movement, the fixed numerical mesh must be greater than the mesh covering the original body.

Paper from: *Structures Under Shock and Impact VII*, N Jones, CA Brebbia and AM Rajendran (Editors).
ISBN 1-85312-911-9

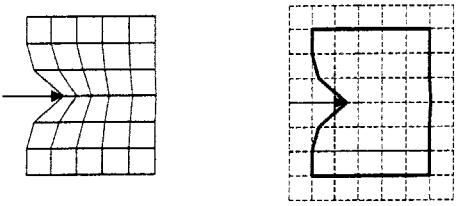

Figure 1: Lagrange (left) and Euler (right) descriptions of material movement

With large displacements, by using Lagrange description of the material movement, numerical problems arise due to distortion and grid tangling of the mesh. This leads to loss of accuracy and can yield small time steps or even terminate the calculation. To overcome the numerical problems, a re-zoning or erosion algorithm can be used. Re-zoning transforms the current numerical mesh into a new numerical mesh. With great distortion or grid tangling, an erosion algorithm must be used to continue the calculation. Erosion is defined as removal of elements in the analysis when a predefined criterion (level) is reached; normally this criterion is taken to be the plastic strain. With the erosion algorithm, a non-physical solution is obtained because internal strain energy is removed from the system. To get realistic solutions, the criterion for erosion – the plastic strain – is normally set above 150% of natural strain.

With the Euler description of the material movement, the problems of distortion and grid tangling are overcome; hence no erosion algorithm is needed.

1.2 Mesh dependency

It is well known that the size of the numerical mesh influences the results, and with a refined mesh the computational time increases dramatically. For dynamic loading the mesh dependency is even more important since more terms are added into the constitutive models. Solutions can be totally invalidated by a poor choice of mesh.

However, there is a risk of having too fine a mesh due to manipulation. To treat the mesh dependency, the common method is to halve the mesh and compare the first coarse mesh with the halved finer mesh; if the results differ negligibly, the analyst is satisfied.

In finite element analyses with dynamic loading, it is important to use several meshes to ensure the accuracy of the results. Moreover, changing a mesh size in the structure must be done with great care. In penetration analyses of projectiles with Lagrange description of the material movement, a rule of thumb is to have at least three elements across the radius of the rod.

By using the Euler description of the material movement, the mesh size must be refined relative to the Lagrange description, due to allowing material movement in the elements.

Paper from: *Structures Under Shock and Impact VII*, N Jones, CA Brebbia and AM Rajendran (Editors).
ISBN 1-85312-911-9

1.3 Residual strength

When a fragment or projectile hits concrete, it will penetrate the concrete. The concrete will be crushed; the strength of the crushed concrete is the residual strength. In a uniaxial stress state, the residual strength is always zero. However, in a multiaxial stress state, as in real structures, the crushed concrete will contribute to the resistance, and therefore have a residual strength. During the penetration, the crushed concrete will be pushed in both longitudinal and lateral directions, consequently giving confinement effects, and stress waves can still propagate through the crushed concrete.

The area under the stress–strain curve is a measurement of the energy absorption of the concrete. The combination of high residual strength and high erosion will lead to more energy absorption than does a lower residual strength with lower erosion.

When studying projectile penetration into concrete, the erosion criterion and the residual strength are important parameters for the result, i.e. the depth of penetration and crater size.

1.4 Strain rate effects

Concrete subjected to impact loading will have an increased strength, both in tension and in compression – the strain rate effect. The increase at high strain rates can be more than a doubling in compression and by more than six times in tension. The increase in tension is as important as the increase in compression. During the penetration of the projectile, the concrete will be compressed in both the longitudinal and radial directions. Due to the compression in the radial direction, a tensile ring will be created around the projectile that holds the concrete together; therefore the increase in tensile strength is important.

2 Experimental test setup

Numerical results presented in this paper are compared to experimental results presented by Hansson [1] and Forrestal *et al.* [2].

In [1] a 6.28-kg steel projectile is used with a length of 225 mm, a diameter of 75 mm, density of 7830 kg/m^3, bulk modulus of 159 GPa, shear modulus of 81.8 GPa, and yield stress of 792 MPa. The target was a concrete cylinder cast in a steel culvert with a diameter of 1.6 m and a length of 2 m. The concrete cube strength was approximately 40 MPa (tested on a 150-mm cube). Two shots were made and the results are shown in Table 1.

Paper from: *Structures Under Shock and Impact VII*, N Jones, CA Brebbia and AM Rajendran (Editors).
ISBN 1-85312-911-9

Table 1. Data summary for the projectile mass and striking velocity, V_s, unconfined uniaxial compressive strength $f'_{c,cube}$ and depth of penetration, *dop*. Experimental results from [1]

V_s (m/s)	Projectile mass (kg)	$f'_{c,cube}$ (MPa)	*dop* (m)
485	6.28	40	0.655 - 0.660*

* Two shots were made, first with supported backside and secondly without support at the backside of the target.

In [2], projectiles made from 4,340 steel rods and heat-treated to a hardness of R_c 43-45 were used. Moreover, filler material was used in the projectiles with a density of 1580 kg/m^3. The projectile length, *l*, was 242.4 mm; its diameter, *d*, was 26.9 mm and the ogival radius, *s*, was 53.8 mm.

The concrete targets were cast in galvanized, corrugated steel culverts with diameter of 1.37 m and target length of 0.76 m for the shot with a striking velocity of 277 m/s. For the two other experiments with impact velocities of 642 and 800 m/s, the target diameter was 1.22 m and the length 1.83 m. The concrete had a density of 2370 kg/m^3 and the unconfined uniaxial compressive cylinder strength varied between 32.4 and 35.2 MPa. Totally three experiments are compared in this paper. The results of these experiments are summarized in Table 2.

Table 2. Data summary for the projectile mass and striking velocities, V_s, unconfined uniaxial compressive strength f'_c and depth of penetration, *dop*. Experimental results from [2]

V_s (m/s)	Projectile mass (kg)	f'_c (MPa)	*dop* (m)
277	0.906	35.2	0.173
642	0.905	34.7	0.620
800	0.904	32.4	0.958

3 Finite element model

3.1 Governing equations

The governing equations in AUTODYN [3] are the Rankine-Hugoniot equations, i.e. conservation of mass, momentum and energy; see Equations 1-3.

Paper from: *Structures Under Shock and Impact VII*, N Jones, CA Brebbia and AM Rajendran (Editors).
ISBN 1-85312-911-9

Conservation of mass:

$$m = \rho_0 V_0 = \rho_1 V_1 \tag{1}$$

Conservation of momentum:

$$m(v_0 - v_1) = p_1 - p_0 \tag{2}$$

Conservation of energy:

$$e_1 - e_0 = 1/2(p_1 + p_0)(V_0 - V_1) \tag{3}$$

Here m is the mass, ρ is the density, V is the volume in equation 1 and specific volume in equation 3, v is the velocity, e is the internal energy and p is the pressure.

To complete the description of the continuum, two further relations describing the material behavior are required: first the equation of state (EOS) and secondly a constitutive model.

3.2 Equation of State (EOS)

The equation of state used in the model is a combined P-Alpha equation of state and a polynomial equation of state.

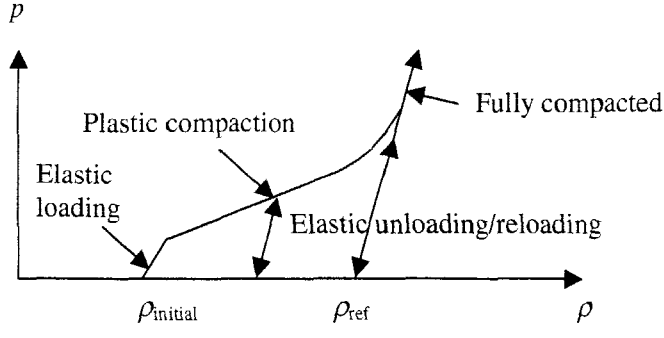

Figure 2: Equation of state

3.3 Constitutive model

The constitutive model used in the study is the RHT model (see Figure 3), developed by Riedel, Hiermaier and Thoma [4]. The RHT model was developed for concrete, but can be used for other brittle materials as well. The model includes pressure hardening, strain hardening, strain rate hardening, third-invariant dependence for compressive and tensile meridians, and a damage model for model strain softening.

Paper from: *Structures Under Shock and Impact VII*, N Jones, CA Brebbia and AM Rajendran (Editors).
ISBN 1-85312-911-9

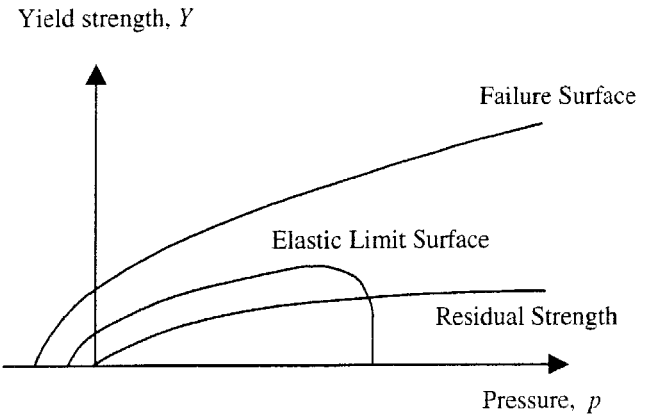

Figure 3: The RHT model

3.4 Numerical mesh

3.4.1 Numerical mesh 1

The numerical mesh 1 is shown in Figure 4, where the results from analysis are compared to experiments from [1]. The target is of concrete cast in a steel culvert. The model is axisymmetric, created by quadratic elements with an element length of 12.5 mm, totaling 64 x 160 elements.

For the Eulerian mesh, the mesh size is 128 x 320 elements.

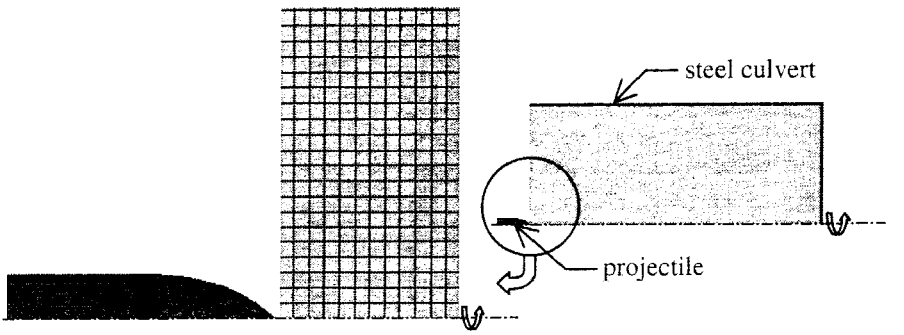

Figure 4: Numerical mesh for experimental setup 1

Paper from: *Structures Under Shock and Impact VII*, N Jones, CA Brebbia and AM Rajendran (Editors).
ISBN 1-85312-911-9

3.4.2 Numerical mesh 2

The numerical mesh 2 is shown in Figure 5, where the results from analysis are compared to experiments from [2]. The target is of concrete cast in a galvanized steel culvert. The model is axisymmetric, created by rectangular elements with an element length of approximately 4 mm. For a target length of 0.76 m the mesh size is 190 x 172 elements as seen in Figure 5, and for the target length of 1.83 m the mesh size is 153 x 458 elements.

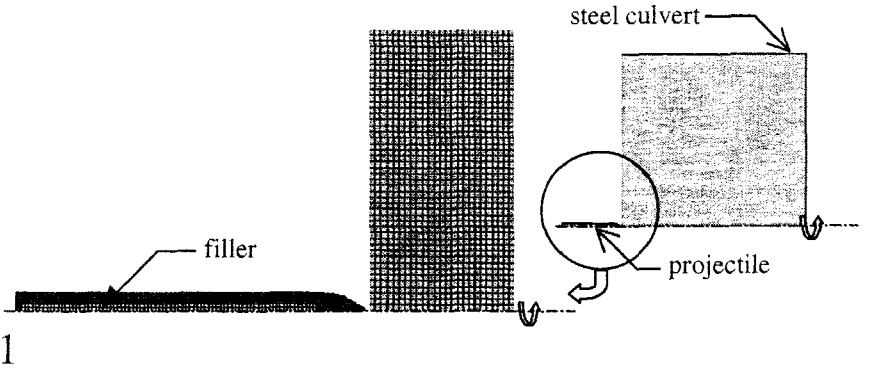

Figure 5: Numerical mesh for experimental setup 2

4 Results

For the experimental results from [1], the crater size and depth of penetration have been compared. Both Lagrangian and Eulerian analyses have been compared to the experimental results. For the experimental results from [2] the depth of penetration has been compared only with the Lagrangian technique.

4.1 Experimental setup 1

The RHT model in AUTODYN was calibrated for the experimental results 1. In the experiment two shots were made, first one with support and secondly one without any support at the backside. The depths of penetration were 655 mm and 660 mm respectively.

The depth of penetration was 653 mm with the Lagrangian technique, and 652 mm with the Eulerian technique, as shown in Figure 6 (difference less than 0.5 %). The dark area is the damage when the projectile velocity is zero. The crater diameter in the analysis is smaller than in the experimental results, where the crater diameter was approximately 0.8 m.

Paper from: *Structures Under Shock and Impact VII*, N Jones, CA Brebbia and AM Rajendran (Editors).
ISBN 1-85312-911-9

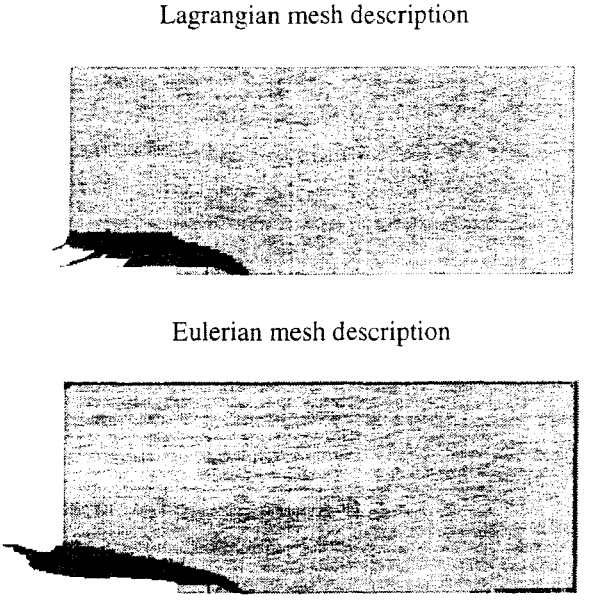

Figure 6: Cratering and the depth of penetration. Above: Lagrangian mesh. Below: Eulerian mesh. Comparison with experiments [1]

4.2 Experimental setup 2

In the numerical model used for comparison with experimental setup 2, the material parameters (strain rate dependency, residual strength, and criteria for erosion) for the concrete target are the same as in experimental setup 1, except for the uniaxial compressive strength and density. Totally three experimental results have been compared, all with a projectile diameter of 26.9 mm, and with varying impact velocities. The results from the analysis are shown in Figure 7, where the depth of penetration is analyzed with the RHT model for different impact velocities.

The yield strength for the R_c 43-45 steel is 972 MPa and the ultimate strength is 1448 MPa. In the numerical model, a Von Mises material model is used for the steel. Since the Von Mises material model has no hardening, the yield strengths of 972 MPa and 1448 MPa were used in the analyses; this gives a lower and an upper limit of the depth of penetration (according to the steel model).

By using the model that was calibrated to experimental results from [1] the model can predict the depth of penetration for high velocities for the experimental results from [2], but not at low impact velocities. New calibration with both experimental results was made; by increasing the criteria for erosion. In figure 7 are the results shown for experiments [2] and for experiment [1] the depth of penetration in the analysis was 622 mm (difference 5 %).

Paper from: *Structures Under Shock and Impact VII*, N Jones, CA Brebbia and AM Rajendran (Editors).
ISBN 1-85312-911-9

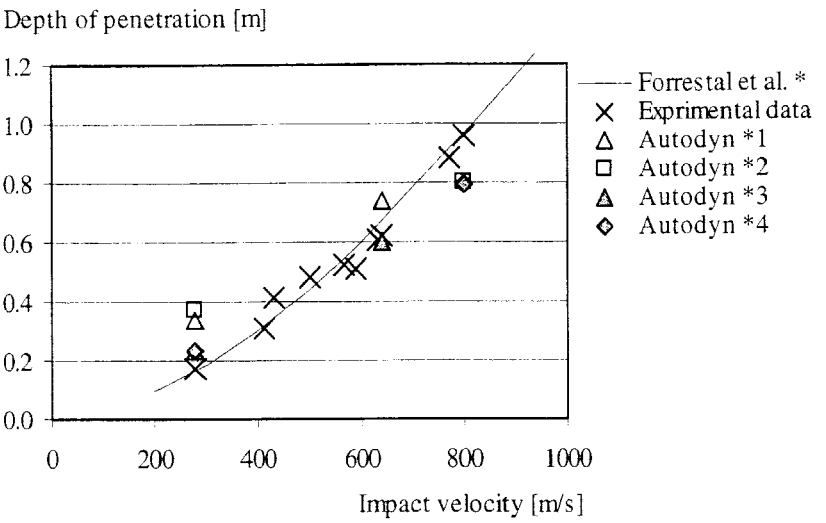

* Empirical equation from [2].
*1 Yield strength for the steel = 972 MPa.
*2 Yield strength for the steel = 1448 MPa.
*3 Yield strength for the steel = 972 MPa, increased criteria for erosion.
*4 Yield strength for the steel = 1448 MPa, increased criteria for erosion.

Figure 7: Comparison of numerical results from RHT model in AUTODYN with experimental results from [2]

5 Conclusions and discussion

Two experimental setups have been compared with finite element analyses in AUTODYN. The Lagrangian and Eulerian techniques are used and compared.

To ensure that the depth of penetration is predicted accurately, several experimental setups must be compared with different impact velocities. In this paper the RHT model in AUTODYN is used for two different experiments with various impact velocities.

The depth of penetration was calibrated against the experimental result from [1]. Thereafter, further analyses with the model were made by comparison with another experimental setup from [2].

The RHT model is capable of predicting the depth of penetration both for the experimental setup 1 and with high impact velocities for the experimental setup 2. For the latter, the depth of penetration was overestimated at low impact velocity. A new calibration was made taking account both experimental setups and as shown in figure 7, the results were improved according to the depth of penetration.

When using the Lagrangian technique, an erosion algorithm must be used to avoid grid tangling and distortion. Consequently, strain energy is removed from the system. By using high criteria (levels) for erosion, the result becomes

Paper from: *Structures Under Shock and Impact VII*, N Jones, CA Brebbia and AM Rajendran (Editors).
ISBN 1-85312-911-9

realistic. The crater size is smaller than for the experimental results. One possible explanation is that the concrete is modeled as a homogeneous material in the model.

The advantage of the Eulerian technique is that no erosion algorithm is needed and therefore no strain energy is removed from the system. In this paper, one experimental result has been compared with the RHT model in AUTODYN. The depth of penetration was predicted for that experiment, but the crater size was smaller than in the experiment.

Acknowledgements

The authors wish to thank the reference group members of the project "Dynamic behaviour of concrete structures subjected to blast and fragments"; Björn Ekengren, M.Sc., from the Swedish Rescue Services Agency, Dr. Mario Plos from Chalmers University of Technology, and Dr. Morgan Johansson from Reinertsen AB.

References

[1] Hansson, H, Numerical simulation of concrete penetration. FOA (Swedish Defence Research Agency), Sweden, July 1998.
[2] Forrestal, M. J., Altman, B. S., Cargile, J. D. and Hanchak, S. J., An empirical equation for penetration depth of ogive-nose projectiles into concrete targets. Int. J. Impact Engng Vol. 15, No. 4, pp. 395-405, 1994.
[3] AUTODYN Theory Manual, Century Dynamics, 2001.
[4] Riedel, W., Thoma, K., Hiermaier, S. and Schmolinske, E. Penetration of Reinforced Concrete by BETA-B-500, Numerical Analysis using a New Macroscopic Concrete Model for Hydrocodes.